Direct observation of individual RecA filaments assembling on single DNA molecules

Roberto Galletto[1,2,3], Ichiro Amitani[1,2,3], Ronald J.Baskin[2] & Stephen C. Kowalczykowski[1,2,3]

Sections of Microbiology[1] and of Molecular and Cellular Biology[2], Center for Genetics and Development[3], University of California, Davis, California 95616, USA

Supplementary Figures and Legends.

The initial stages of the RecA filament formation on double-stranded DNA

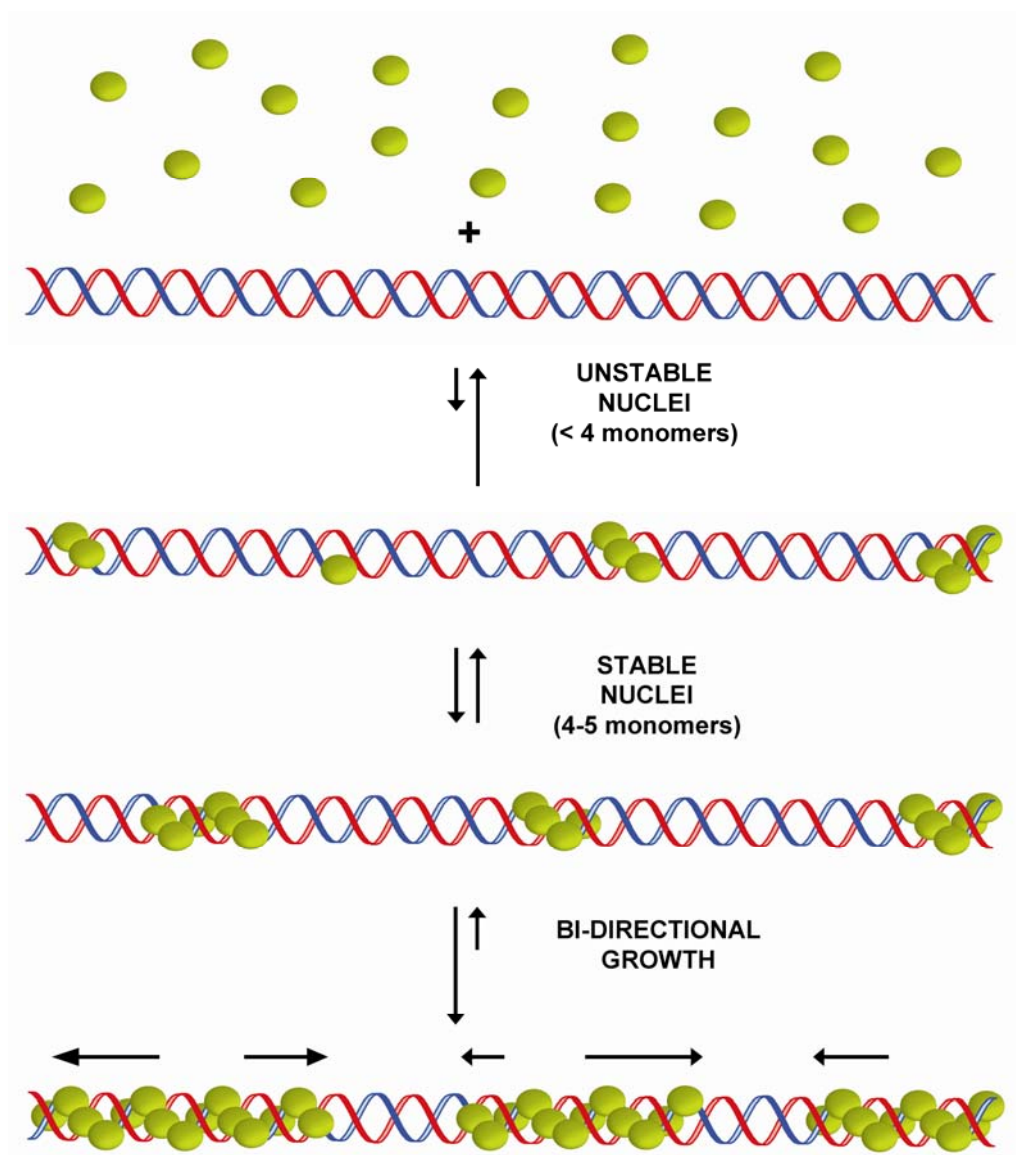(dsDNA) are schematically depicted in Fig. S1. The initial nucleation of RecA protein on

Figure S1. Schematic representation of RecA filament formation on dsDNA.

dsDNA occurs at multiple positions on the nucleic acid lattice, preferentially at regions of

high AT sequence content. The binding of up to ≈ 4 RecA monomers to the dsDNA does

not lead to stable interactions, and the unstable nuclei dissociate back into solution.

Binding of 4-5 RecA monomers is required for the formation of a stable nucleus. Once

stable RecA nuclei are formed, filaments grow bidirectionally by addition of monomers

at both ends of the nascent clusters.

Analysis

The instrumental set-up was essentially as reported[31-33], with minor modifications

noted in the Methods. Images were recorded by a CCD camera (EB-CCD C7190-23;

Hamamatsu Photonics, Hamamatsu, Japan), digitalized at 20-30 frames per second, and

further processed using ImageJ software (NIH). All time averaged images are from 10

sec of observation. The position of each observed cluster along the λ DNA molecule was

measured with respect to the center of the bead and normalized to the original observed

dsDNA length. Under the experimental conditions employed, the observed length of the

λ DNA prior to YOYO-1 dissociation is 13.6 ± 0.4 μm. For all experiments monitoring

the growth of individual clusters, time zero is defined as the first time of appearance of a

distinguishable cluster. The length of the observed clusters was determined from the

difference of the distances of left and right side relative to bead. In the experiment where

directionality is monitored, the absolute distance of the left and right side of the cluster

relative to the bead center is reported. Error bars represent the standard deviation for data

shown.

Fluorescent labeling of RecA

Wild type RecA protein was purified as previously described[34]. Chemical

modification of RecA was performed by coupling carboxyfluorescein to amines at pH

7.0. Because of the large difference in pK_a between the terminal α-amino group and the

ε-amino group of lysine, the amino-terminus of the protein will be preferentially

labeled[35]. RecA at concentrations of 2-4 mg/ml in Buffer L (50 mM K_2HPO_4/KH_2PO_4 pH

7.0, 1 M NaCl, 0.1 mM DTT, 10% v/v glycerol) was reacted with a 12-fold molar excess

of 5(6)-carboxyfluorescein, succinimidyl ester (Molecular Probes, Eugene, OR) for 4

hours at 4 °C in the dark and then the reaction stopped with 50 mM Tris-HCl pH 7.5.

Unreacted fluorescent label was separated from carboxyfluorescein modified RecA using

a Bio-Gel P10 (Bio-Rad Laboratories, Richmond, CA) column. The degree of labeling of

the RecA protein, as determined from UV-VIS spectrophotometric ratios utilizing

ε_{492}=78000 M^{-1} cm^{-1} (pH 9), is 0.8-1.2. For different preparations, the degree of labeling

was 0.8-1.2, consistent with a single label per protein molecule on average.

Fluorescent RecA is fully active

The single-stranded DNA (ssDNA) dependent ATPase activity of

carboxyfluorescein-labeled RecA (RecA^f) is shown in Fig. S2 compared to that of

unlabeled RecA. Within experimental error, both the maximum rate of ATP hydrolysis

and the stoichiometry at DNA saturation for RecA^f are indistinguishable from the
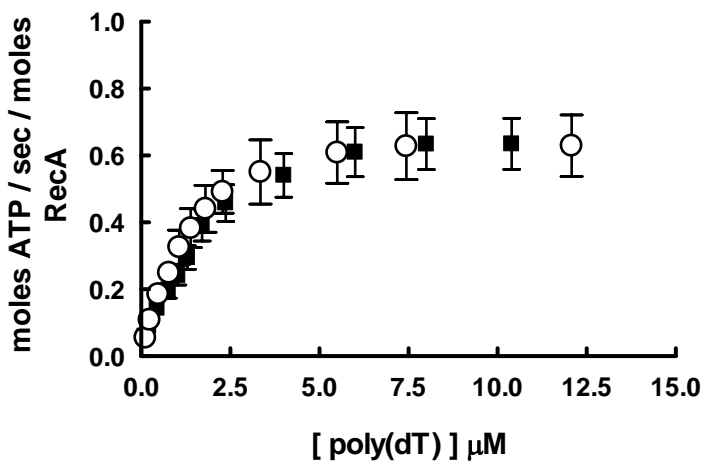
unlabeled protein.

Figure S2. ATP hydrolysis was measured spectrophotometrically with an enzyme-linked assay in 25 mM Tris-Acetate (pH 7.5), 8 mM Mg(OAc)$_2$, 1 mM DTT, 1 mM ATP, 1.5 mM PEP, 35 U/mL PK, 20 U/mL LDH, 0.2 mg/mL NADH, and 0.5 μM RecA (closed squares) or RecA^f (open circles) at 37 °C.

Another hallmark of RecA function is stimulation by the ssDNA-binding protein (SSB). The ability of SSB to stimulate the ATP hydrolysis of RecA[f] was tested on circular M13 mp7 ssDNA. In Fig. S3, the change in the rate of ATP hydrolysis is shown
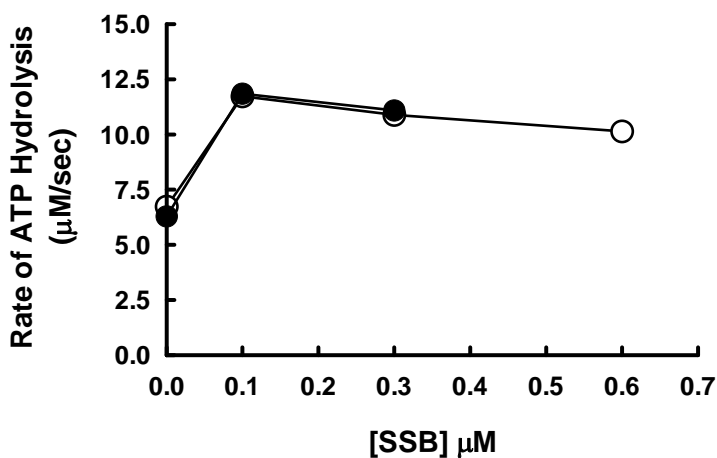

Figure S3. Stimulation of ATPase activity of RecA by SSB was measured using the same conditions as in Fig. S1, except that ssDNA M13mp7 (1.5 µM nt) was used; the RecA concentration was 0.5 µM. SSB was added 2' after initiation of reaction. RecA, closed circles; RecA[f], open circles.

as function of SSB concentration. Both unlabeled and labeled RecA show a ~2-fold maximal increase in rate over the same range of SSB concentration, consistent with expectations[36, 37]. Thus, RecA[f] can form fully active filaments on ssDNA which display ATP hydrolysis that is indistinguishable from unlabeled RecA.

Finally, the ability of RecA[f] to catalyze DNA strand exchange between circular ssDNA and linear dsDNA substrate was examined (Fig. S4). The ability of RecA[f] to promote DNA strand exchange to form nicked circular DNA products shows that the fluorescent label does not interfere with the ability of RecA to catalyze DNA pairing or strand exchange. Thus, these assays indicate that RecA[f] is not altered by the chemical labeling.
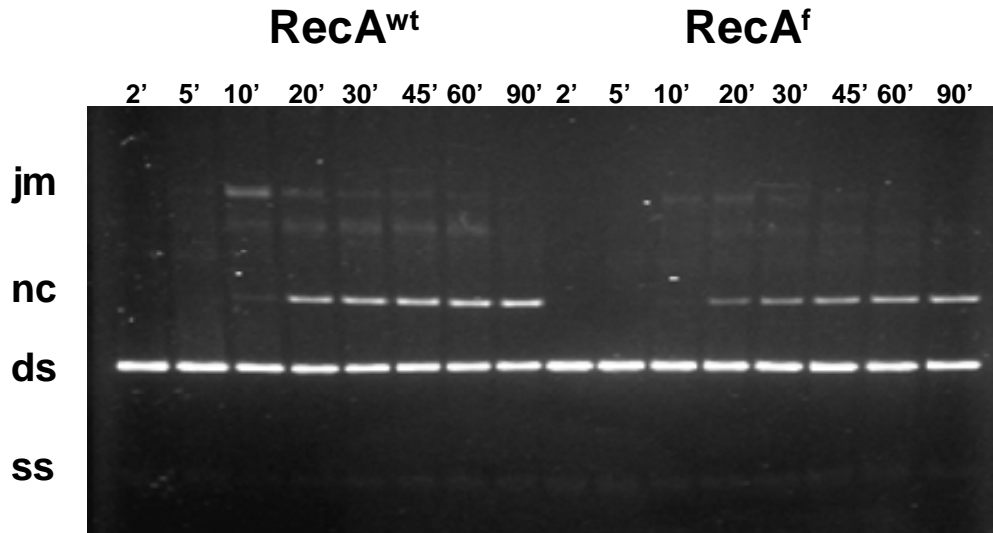
RecA^wt   **RecA^f**

2'   5' 10' 20' 30' 45' 60' 90' 2'   5' 10'   20' 30' 45' 60' 90'

jm

nc

ds

ss

Figure S4. RecA or RecA^f at a final concentration of 3 μM was added to 5 μM (nucleotides) φX174 ssDNA in Buffer E (25 mM Tris-Ac pH 7.5, 10 mM Mg(OAc)$_2$, 1 mM DTT, 5 mM ATP) and the solution was incubated at 37 °C for 1 min, followed by addition of SSB to a final concentration of 0.45 μM and incubated 1 min further. DNA strand exchange was initiated by addition of 10 μM (nucleotides) linearized φX174 dsDNA. At the indicated times, a 10 μL aliquot of the reaction was stopped with addition of 5X stop solution (25% glycerol, 0.1 mM EDTA, 10% SDS, 0.1 mg/mL bromophenol blue and 0.1 mg/mL xylene-cyanol). The products of reaction were resolved by agarose gel (1%) electrophoresis, then stained with ethidium bromide, and visualized with a Fluorochem^TM 8900 (Alpha Innotech): jm, joint molecules; nc, nicked circular DNA; ds, double-stranded DNA; ss, single-stranded DNA.

RecA-ATPγS filaments are highly stable

Fluorescent RecA filaments, which were formed in presence of ATPγS at low pH and shifted to high pH in the absence of any free ATPγS, remain stably associated with the DNA for at least 20 min (Fig. 1b). To further address the stability of the ATPγS-RecA-dsDNA complex, individual filaments were incubated in 1 M NaCl in the observation channel (Fig. S5, Panel A). No dissociation is evident for up to 8 min. These results suggest that the ATPγS-RecA complex in the filament is locked in a conformation where the nucleotide cannot be released from the complex, resulting in a stable filament. Thus, not only does ATPγS induce a high-affinity DNA-binding state of RecA, but neither ATPγS nor the ATPγS-RecA complex can be dissociated from the DNA.

The stability of the bound nucleotide within RecA filaments was also confirmed by its inability to exchange with free ATP in solution. When preformed RecA-ATPγS filaments were relocated into the observation channel containing 1 mM ATP, no apparent dissociation occurs for at least 7 min (Fig. S5, Panel B). If ATPγS had exchanged with the ATP in solution, the RecA would dissociate due to ATP hydrolysis. The observation that ATPγS cannot be exchanged and that no detectable dissociation occurs shows that extensive ATPγS hydrolysis does not occur within the RecA filament.
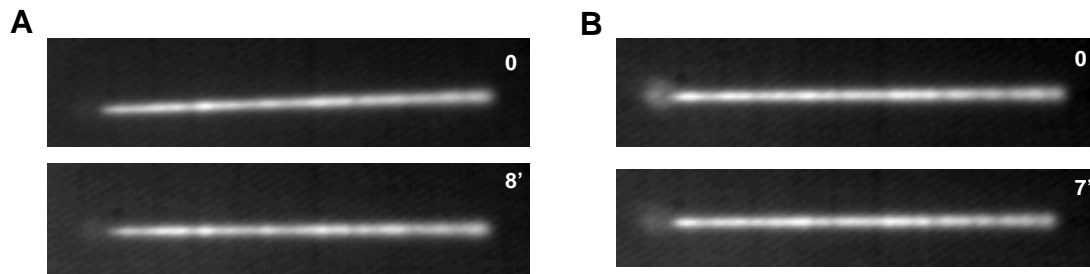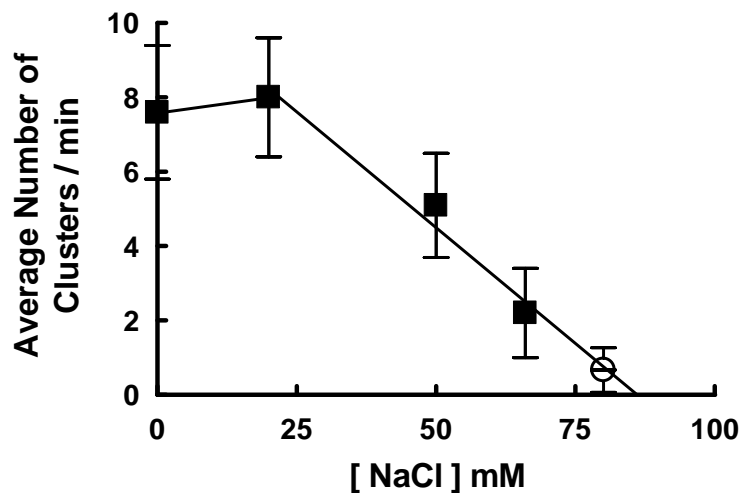
A

B

Figure S5. A. RecA-ATPγS filaments in 1 M NaCl, at the beginning of incubation and after 8' in the observation channel with constant flow, but with illumination off. **B.** RecA-ATPγS filaments in 1 mM ATP, at the beginning of incubation and after 7' in the observation channel with constant flow, but with illumination off.
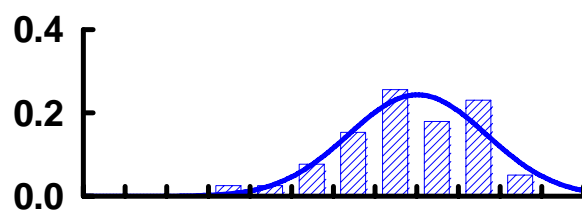
At high NaCl concentrations, nucleation becomes a rate-limiting step for RecA assembly

Several bulk phase studies suggested that nucleation frequency decreases at increased concentrations of salt [38-41]. To determine whether this was indeed the case, and to define conditions where nucleation might be limited to one nucleus, the same dipping protocol (Fig. 1d) was used at various NaCl concentrations. The average number of RecA clusters reported in the distributions of Fig. 1d is shown as function of NaCl concentration in Fig. S6. The frequency of cluster formation is highly salt concentration-
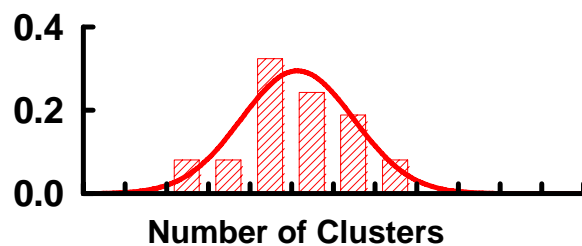
A

B

C

Figure S6. A. Salt concentration dependence for the average number of clusters formed in 1 minute. Standard deviation is from 20-40 molecules; to observe a sufficient number of clusters at 80 mM NaCl (open circle), the observation time was increased to 3 minutes. Distribution of the observed number of clusters at 20 mM (B) and 50 mM (C) NaCl, with a bin size of 1. The solid lines are Gaussian fits of the data. Data for 0 and 66 mM NaCl appear in Fig 1e.

dependent and at higher concentrations, nucleation becomes limiting. Indeed, compared

to 66 mM NaCl, to detect a comparable number of clusters at 80 mM NaCl, it was

necessary to increase the time of incubation in the RecA-channel by 3-fold.

A nucleation bias is revealed at elevated NaCl concentrations: RecA preferentially nucleates at AT-rich DNA

To determine where RecA filaments nucleate, we examined the locations of cluster formation along λ DNA. At low concentration of NaCl (20 mM), the distribution of RecA clusters does not reveal any preference for specific positions along the lattice, except at the end of the DNA molecule which has a 12 nucleotide 5'-ssDNA end (Fig. S7). Under these conditions, the nucleation frequency is high (Fig. 1d and Fig. S6), and nucleation is equally probable at all dsDNA sites.
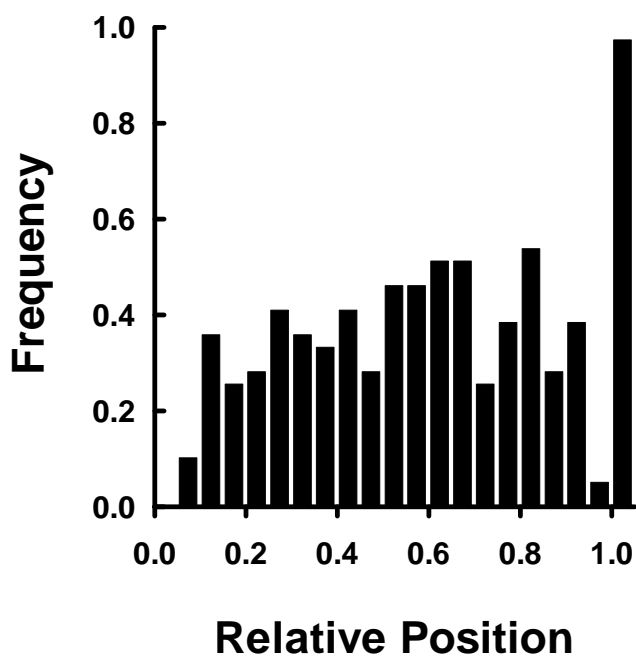
Figure S7. Distribution of clusters along λ DNA obtained at 20 mM NaCl (N=40).

However, when the nucleation frequency is reduced by elevating the NaCl concentration (to 66 mM) (Fig. 1d and Fig. S6), a preference is revealed. When the distribution frequency is compared to the AT-content of λ DNA, two features emerge (Fig. S8). First, a large fraction of molecules has a cluster at the right end of the λ DNA, showing a preference for the 12 nucleotide 5'-ssDNA tail in λ DNA; this preference is

consistent with the higher affinity of RecA protein for ssDNA[39, 42]. Interestingly, the RecA clusters that formed at the end are not larger than those that formed at internal positions, even though the ssDNA tail is in the proper orientation (5'→3') to allow for filament growth[43-45]. If RecA filaments could indeed grow rapidly from rate-limiting nuclei, then the end cluster should be, on average, larger than any other cluster. Thus, under these conditions, growth from an individual cluster is limited and filament formation occurs *via* multiple nucleation events. The second feature is that clusters show a preference for the rightmost half of λ DNA, which is AT-rich.
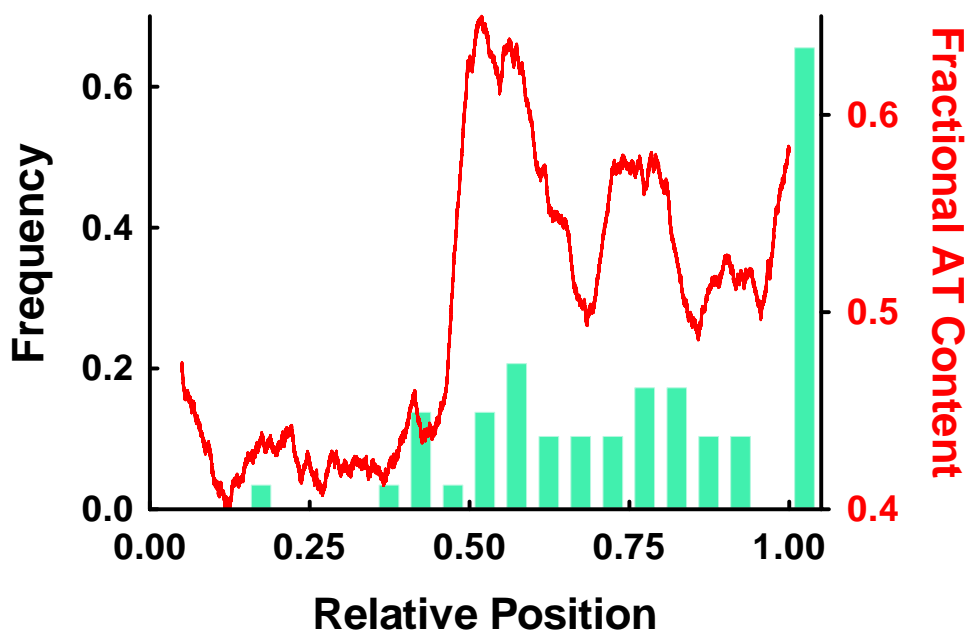

Figure S8. RecA clusters nucleate preferentially at the ssDNA tail and AT-rich regions of λ DNA. The locations of the RecA clusters measured in Fig. 1d are plotted *versus* their relative position along λ DNA (green bars). The solid red line is the AT-content, calculated with a bin size of 5%.

The preference for the rightmost side of λ DNA is even more evident when the data are plotted with a 50% bin size and the end clusters are excluded to avoid a bias due to the ssDNA end (Fig. S9A). To eliminate any potential contributions to this bias from flow, the orientation of the λ DNA was also inverted by attaching it to the bead *via* a biotinylated oligonucleotide complementary to the *cosR* end. Utilizing this oppositely

oriented λ DNA, with the AT-rich region now positioned close to the bead, RecA clusters were now observed more frequently at the leftmost side of the λ DNA (Fig. S9B). The same experiments utilizing λ DNA attached in both orientations were also performed at 80 mM NaCl, and the same result was obtained (Fig. S9C and D).

When the data obtained from each of the oppositely oriented λ DNA molecules are combined (Fig. S10), a statistically significant preference for RecA cluster formation
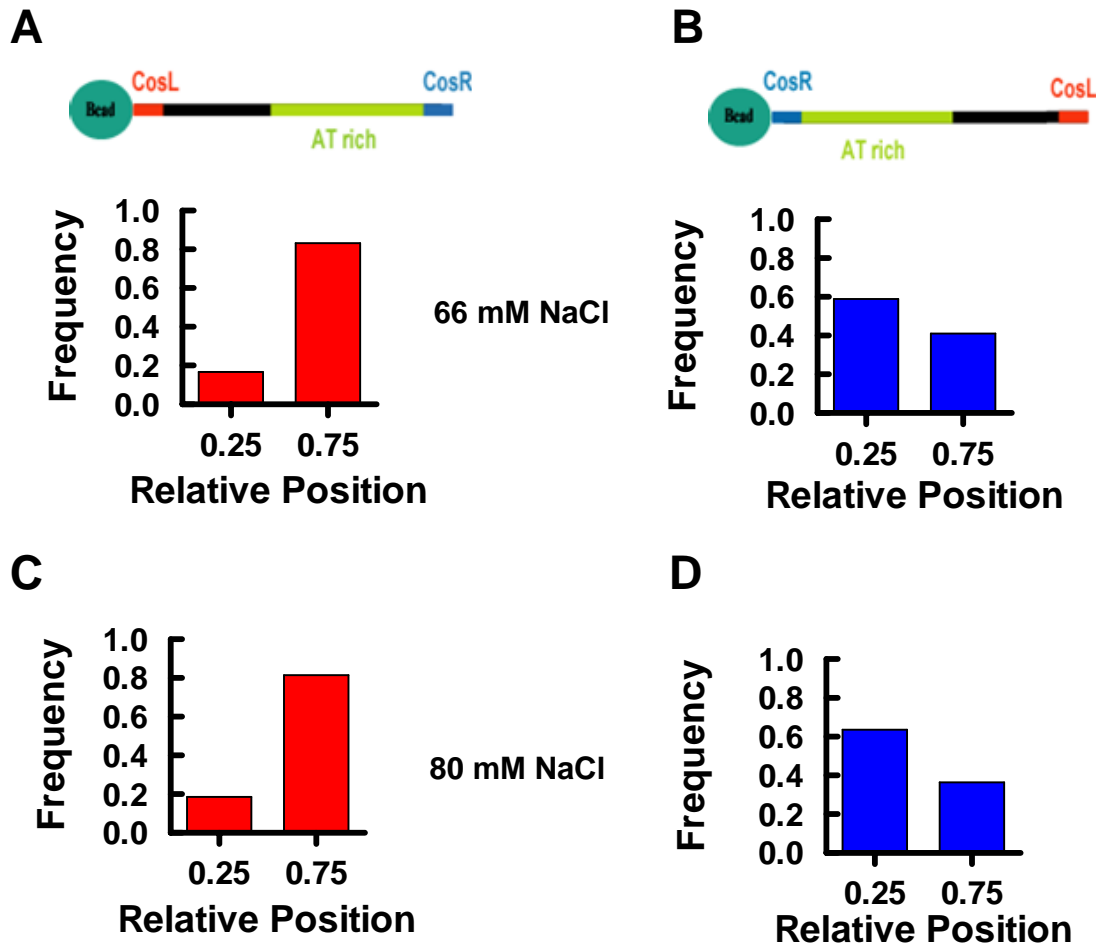
A

CosL   **CosR**

Bead

AT rich

66 mM NaCl

Frequency — Relative Position

B

CosR   **CosL**

Bead

AT rich

Frequency — Relative Position

C

80 mM NaCl

Frequency — Relative Position

D

Frequency — Relative Position

Figure S9. A and B. Cluster distribution along λ DNA obtained at 66 mM NaCl for two different orientations of the λ DNA. C and D. Same experiment as in A and B, but at 80 mM NaCl.

at the AT-rich region of λDNA is evident. This finding is consistent with RecA solution studies[38, 46] and is similar to the preference of MuB protein from bacteriophage Mu[47, 48].
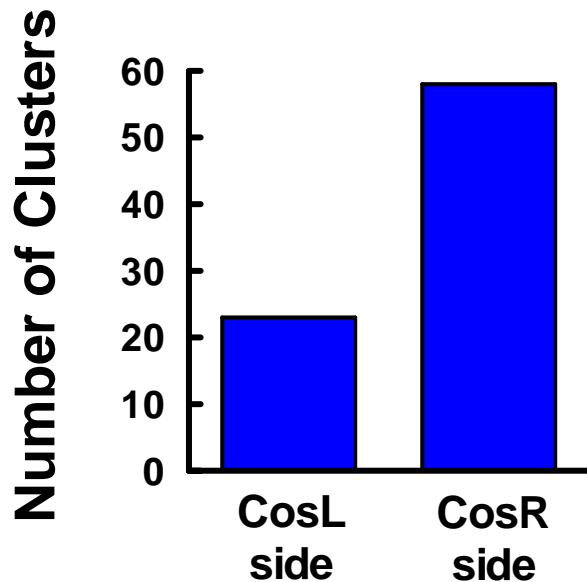
Figure S10. RecA clusters nucleate preferentially at the ssDNA tail and AT-rich regions of λ DNA. Location of RecA clusters on λ DNA, combining experiments where the DNA was attached to beads in opposite orientations (see Fig. S9). The histogram uses a bin size of 50%, and clusters at the ssDNA end are excluded; χ^2=15.1 and p=0.0001.

Relationship between DNA elongation and RecA filament formation

The growth of RecA filaments can also be determined from the change in length of filaments as function of time. An example is shown in the Fig. S11, for a RecA filament formed in the presence of ATP and no NaCl. As previously reported[49-52], the time trace is characterized by an initial lag phase followed by linear extension until saturation of DNA with RecA is achieved. The linear growth phase shows multiple growing clusters (Fig. S11). The average rate of growth determined from the linear phase is 31.8 ± 8.7 nm s^{-1} (N=8) (or ~20 RecA monomer s^{-1}). However, this rate is only an apparent value because the observed extension of the DNA molecule originates from the multiple clusters whose number changes over time. Thus, the observed rate of growth measured from the linear phase is a combination of both the nucleation frequency and the growth rate of a nucleus. Indeed, the average rate of growth determined directly for

individual growing clusters is 10.2 ± 4 nm s^{-1} (or ~6 RecA monomer s^{-1}), which is 3 times lower (see Fig. 3c). Thus, analysis of the rate of RecA filament assembly exclusively from the rate of dsDNA extension can lead to overestimates of the growth rate if the observed signal does not originate from a single growing cluster. Previous estimates for the rate of RecA filament growth from the change of dsDNA extension as function of time, provided estimates for growth in the range of 10-20 RecA monomers s^{-1} [49-52]. Growth rates as high as 25 monomers s^{-1} [51], and slow as ≈ 3 s^{-1} were also reported[53].
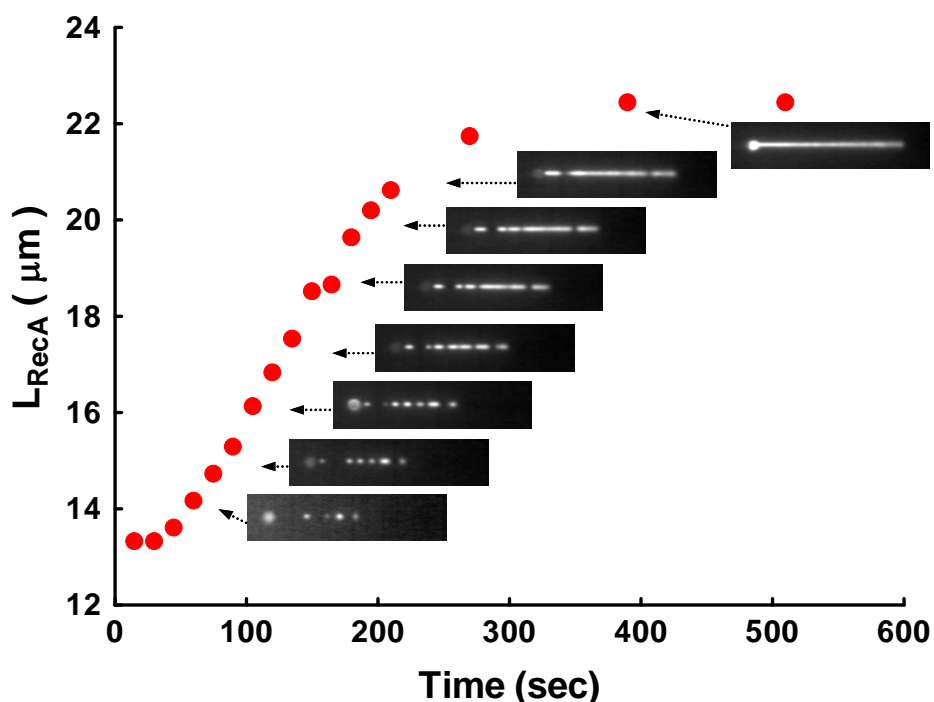

Figure S11. A comparison of RecA filament formation and changes in the observed DNA length**.** The length of a DNA molecule as a function of incubation time, with corresponding time averaged images as a function of total incubation time for 170 nM RecA, 0.5 mM ATP, 1 mM Mg(OAc)$_2$ and stabilized with 5 mM ATP/10mM CaCl$_2$. The rate of RecA filament growth is calculated from the slope of the linear phase.

Stabilization of ATP-RecA clusters by Ca^{2+} ions

While RecA clusters formed in the presence of ATPγS show a high stability, those formed in the presence of an equal amount of ATP completely dissociated in ≈ 6 min after a lag of ≈ 10-20 sec (unpublished observations). Unstable RecA-ATP clusters

can be "frozen" in the observation channel if ATPγS is present in solution, indicating that bound ATP can be quickly exchanged for the non-hydrolysable, higher affinity analog. However, we found that the RecA-ATP clusters formed in the presence of Mg^{2+} ions can also be stabilized in the observation channel by high concentrations of ATP and $CaCl_2$. A partial RecA filament that was stabilized in the observation channel by the presence of 10 mM ATP and 5 mM $CaCl_2$ is shown in Fig. S12. It is evident that in the 10 second observation time used for these experiments no apparent extensive dissociation occurs. Indeed, aside from partial photobleaching, clusters do not undergo major dissociation up to 60 sec.
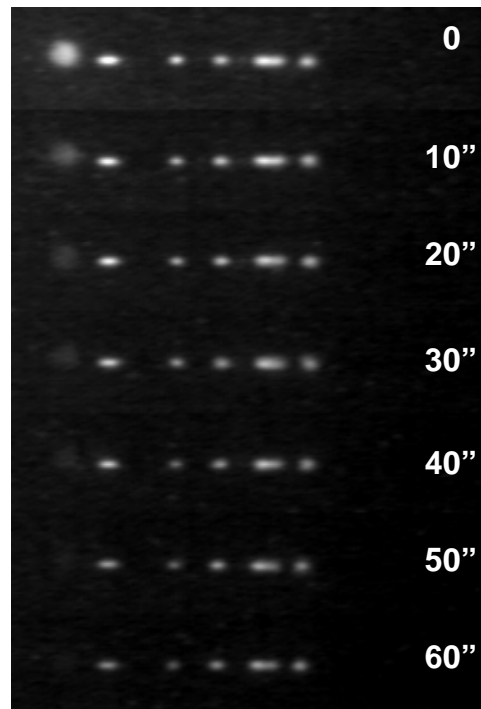

Figure S12. ATP-RecA clusters on dsDNA can be transiently stabilized. The stability of RecA clusters stabilized in the observation channel with 10 mM ATP and 5 mM $CaCl_2$ is shown as a function of time.
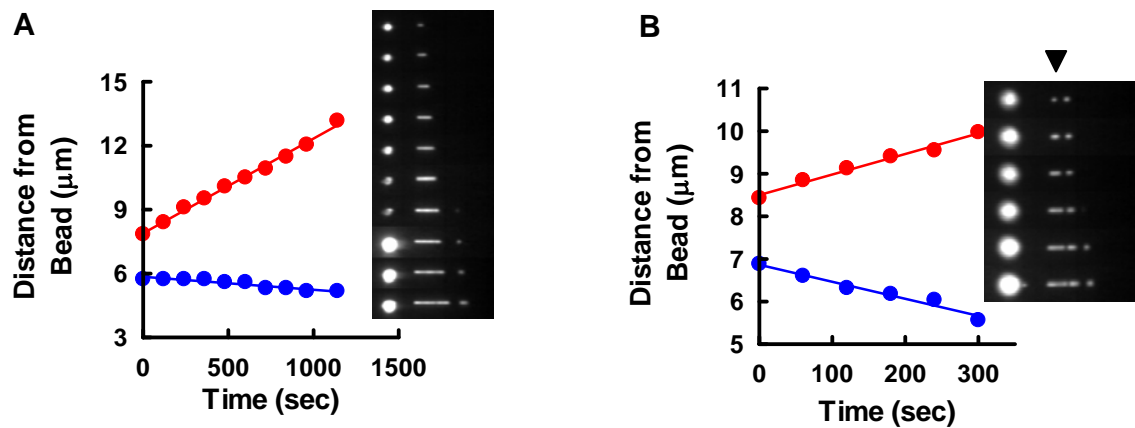
Examples of unidirectional *versus* bidirectional RecA nucleoprotein filament growth

Fig. S13. RecA filaments can grow either unidirectionally (A) or bidirectionally (B) in the presence of ATP. Red and blue symbols represent the growing right and left edges of the clusters, respectively. The solid lines are linear fits of the data. The arrow in C points to the cluster measured.

Supplementary Notes.

31.   Bianco, P. R. et al. Processive translocation and DNA unwinding by individual RecBCD enzyme molecules. Nature 409, 374-378 (2001).

32.   Spies, M. et al. A molecular throttle: the recombination hotspot χ controls DNA translocation by the RecBCD helicase. Cell 114, 647-54 (2003).

33.   Handa, N., Bianco, P. R., Baskin, R. J. & Kowalczykowski, S. C. Direct visualization of RecBCD movement reveals cotranslocation of the RecD motor after χ recognition. Mol. Cell 17, 745-50 (2005).

34.   Mirshad, J. K. & Kowalczykowski, S. C. Biochemical basis of the constitutive coprotease activity of RecA P67W protein. Biochemistry 42, 5937-44 (2003).

35.   Kim, Y. T., Tabor, S., Churchich, J. E. & Richardson, C. C. Interactions of gene 2.5 protein and DNA polymerase of bacteriophage T7. J Biol Chem 267, 15032-40 (1992).

36.   Kowalczykowski, S. C. & Krupp, R. A. Effects of *Escherichia coli* SSB protein on the single-stranded DNA-dependent ATPase activity of *Escherichia coli* RecA protein: Evidence that SSB protein facilitates the binding of RecA protein to regions of secondary structure within single-stranded DNA. J. Mol. Biol. 193, 97-113 (1987).

37.   Kowalczykowski, S. C., Clow, J., Somani, R. & Varghese, A. Effects of the *Escherichia coli* SSB protein on the binding of *Escherichia coli* RecA protein to

single-stranded DNA: Demonstration of competitive binding and the lack of a specific protein-protein interaction. J. Mol. Biol. 193, 81-95 (1987).

38.   Kowalczykowski, S. C., Clow, J. & Krupp, R. A. Properties of the duplex DNA-dependent ATPase activity of *Escherichia coli* recA protein and its role in branch migration. Proc. Natl. Acad. Sci. U. S. A. 84, 3127-3131 (1987).

39.   McEntee, K., Weinstock, G. M. & Lehman, I. R. Binding of the recA protein of *Escherichia coli* to single- and double-stranded DNA. J. Biol. Chem. 256, 8835-8844 (1981).

40.   Chabbert, M., Cazenave, C. & Helene, C. Kinetic studies of recA protein binding to a fluorescent single-stranded polynucleotide. Biochemistry 26, 2218-25 (1987).

41.   Pugh, B. F. & Cox, M. M. General mechanism for RecA protein binding to duplex DNA. J. Mol. Biol. 203, 479-93 (1988).

42.   Menetski, J. P. & Kowalczykowski, S. C. Interaction of recA protein with single-stranded DNA. Quantitative aspects of binding affinity modulation by nucleotide cofactors. J. Mol. Biol. 181, 281-295 (1985).

43.   Register, J. C., III & Griffith, J. The direction of RecA protein assembly onto single strand DNA is the same as the direction of strand assimilation during strand exchange. J. Biol. Chem. 260, 12308-12312 (1985).

44.   Shaner, S. L., Flory, J. & Radding, C. M. The distribution of Escherichia coli recA protein bound to duplex DNA with single-stranded ends. J. Biol. Chem. 262, 9220-30 (1987).

45.   Shaner, S. L. & Radding, C. M. Translocation of Escherichia coli recA protein from a single-stranded tail to contiguous duplex DNA. J. Biol. Chem. 262, 9211-9 (1987).

46.   Bar-Ziv, R. & Libchaber, A. Effects of DNA sequence and structure on binding of RecA to single-stranded DNA. Proc. Natl. Acad. Sci. U. S. A. 98, 9068-73 (2001).

47.   Greene, E. C. & Mizuuchi, K. Direct observation of single MuB polymers: evidence for a DNA-dependent conformational change for generating an active target complex. Mol. Cell 9, 1079-89 (2002).

48.   Greene, E. C. & Mizuuchi, K. Visualizing the assembly and disassembly mechanisms of the MuB transposition targeting complex. J. Biol. Chem. 279, 16736-43 (2004).

49.   Shivashankar, G. V., Feingold, M., Krichevsky, O. & Libchaber, A. RecA polymerization on double-stranded DNA by using single-molecule manipulation: the role of ATP hydrolysis. Proc. Natl. Acad. Sci. U. S. A. 96, 7916-21 (1999).

50.   van der Heijden, T. et al. Torque-limited RecA polymerization on dsDNA. Nucleic Acids Res 33, 2099-105 (2005).

51.   Fulconis, R. et al. Twisting and untwisting a single DNA molecule covered by RecA protein. Biophys. J. 87, 2552-63 (2004).

52.   Hegner, M., Smith, S. B. & Bustamante, C. Polymerization and mechanical properties of single RecA-DNA filaments. Proc. Natl. Acad. Sci. U. S. A. 96, 10109-14 (1999).

53.   Sattin, B. D. & Goh, M. C. Direct observation of the assembly of RecA/DNA complexes by atomic force microscopy. Biophys. J. 87, 3430-6 (2004).